

# Development and Application of Magneto-Optical Microscope Using Polarization-Modulation Technique

Katsuaki Sato<sup>\*,\*\*</sup>, Member  
Takayuki Ishibashi<sup>\*\*\*</sup>, Non-member

Magneto-optical (MO) microscope has been utilized as a powerful tool for visualization of magnetic domains and magnetic flux distributions. In addition, distribution of a magnetic flux diverging from a magnetized sample and/or distribution of a current in the superconducting sample can be visualized with a help of an MO indicator film placed on the sample. In order to obtain quantitative information of the flux distribution we have developed an MO microscope using a polarization modulation technique. Utilizing the MO microscope with a magnetic garnet film as an indicator we have obtained a quantitative image of current distribution in a superconducting film of MgB<sub>2</sub>.

**Keywords** : Magneto-optical effect, Microscope, Polarized light, Polarization modulation, Current distribution, Superconductor

## 1. Introduction

Magneto-optical (MO) microscopes have been used as one of the most significant techniques for an observation of magnetic domain structures in magnetic materials. Recently, this technique attracts great attention as a powerful tool for visualization of invisible phenomena, such as spin-accumulation in nonmagnetic semiconductors<sup>(1),(2)</sup>, magnetic flux intrusion in superconductors<sup>(3)-(5)</sup>, etc. MO microscopes have technical advantages such as a short measuring time, a simple instrumental setup compared with other imaging techniques, e.g., a magnetic force microscope (MFM)<sup>(6)</sup>, a superconducting quantum interference device (SQUID) microscope<sup>(7)</sup> and a Hall-probe microscope<sup>(8)</sup>.

However, conventional MO microscopes using a crossed polarizer setup are not suited for quantitative evaluation of the MO rotation and ellipticity, particularly in inhomogeneous samples. In order to overcome the problem, we have developed an MO microscope based on a new concept of polarization modulation technique. This concept is an extension of the modulation MO spectroscopy using photoelastic modulator (PEM), which modulates an optical retardation sinusoidally<sup>(9),(10)</sup>. Since the conventional PEM operates at high frequency of about 50 kHz, the modulation technique is not directly applicable to image observation using CCD sensors. Instead of PEM modulation we utilize a digital modulation method, in which images of the MO rotation and ellipticity are reconstructed from three sequentially captured optical images taken with three different polarization states; i.e., linearly polarized (LP) light, right circularly-polarized (RCP) light and left circularly-polarized (LCP) light<sup>(11)</sup>.

In addition to an evaluation of MO parameters, MO microscopes can be utilized for a visualization of magnetic flux and/or current distribution in superconductors with a help of MO

indicator films such as Bi-substituted yttrium iron garnet films<sup>(3)-(5)</sup>. A quantitative magnetic flux image is visualized with a help of the MO indicator film, to which a stray magnetic flux diverging from a superconductor is transferred. A quantitative value of magnitude of the magnetic flux can be calibrated using a magnetic field vs. MO characteristics in the indicator film. As indicator films, we used high quality Bi-substituted yttrium iron garnet films with an in-plane magnetization prepared by a metal organic decomposition (MOD) method<sup>(12),(13)</sup>. Combining the MO microscope with this MO indicator film, we have achieved magnetic sensitivity of < 1 mT and spatial resolution of < 1 μm.

## 2. Magneto-Optical Microscope

### 2.1 Polarization Modulation Technique

In our newly-developed system, images of Faraday rotation  $\theta_F$  and Faraday ellipticity  $\eta_F$  can be calculated from three images taken with three different optical polarization states. MO values of each pixel are obtained from equations,

$$\theta_F \approx \frac{1}{2} \left\{ \frac{2I_{LP} - (I_{RCP} + I_{LCP})}{(1 - \eta_F^2)(I_{RCP} + I_{LCP})} \right\}, \dots \dots \dots (1)$$

$$\eta_F \approx \frac{1}{2} \left( \frac{I_{LCP} - I_{RCP}}{I_{LCP} + I_{RCP}} \right), \dots \dots \dots (2)$$

where  $I_{LP}$ ,  $I_{RCP}$  and  $I_{LCP}$  are signal intensities at each pixel of an image sensor for LP, RCP and LCP, respectively. Derivation of equations (1) and (2) is described in detail in ref. (11).

In order to obtain images for LCP, LP and RCP sequentially we used a rotatable quarter wave plate in the first stage of developmet<sup>(14),(15)</sup>. This method, however, takes a few tens of second to get one MO image. We improved the response time in the second stage; we have made use of a liquid crystal modulator (LCM), by which three polarization images for LCP, LP and RCP can be sequentially measured by only applying to the LCM an AC voltage that is appropriate for each polarization state.

\* Graduate School of Engineering, Tokyo University of Agriculture and Technology, Koganei, Tokyo 184-8588, Japan

\*\* Research Supervisor, Japan Science and Technology Agency, Chiyodaku, Tokyo 102-0075, Japan

\*\*\* Department of Materials Science and Technology, Nagaoka University of Technology, Nagaoka, Niigata 940-2188, Japan

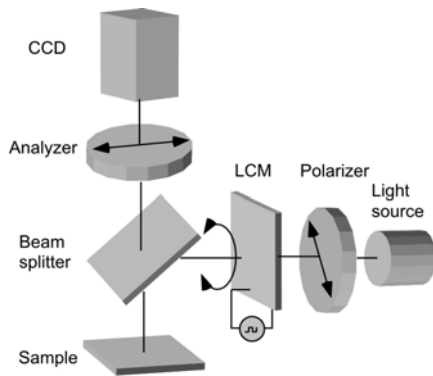


Fig. 1. A schematic drawing of MO microscope using polarization modulation technique.

Figure 1 shows an optical setup of the MO microscope, which we have developed. This system consists of a light source, a polarizer, a liquid crystal modulator (LCM), a beam-splitter, an analyzer and a CCD camera. An objective lenses with a long working distance (Mitsutoyo G Plan APO  $\times 10$ ,  $\times 50$ ) were employed. Digital images of  $640 \times 480$  pixels are taken by a high speed CCD camera (Hamamatsu, C9300-201) with a 12-bit A-D converter, which can directly transfer 160 digital images/sec to RAM in the computer. As a light source, we used either a green light emitting diode (LED) (central wavelength of 530 nm), or a halogen-tungsten lamp equipped with a set of bandpass interference filters for wavelength bands (band-width of 10 nm) at 450, 500, 550, 600, 650 nm. The LCM was prepared using a commercially available liquid crystal (ZLI-4792) and ITO-coated glass plates. The retardation was varied by an application of AC voltage of 0 - 10 V with a frequency of approximately 100 Hz to the LCM in this experiment. Using this system, MO images can be displayed at a rate of approximately 1 frame/sec using 20 optical images taken with a exposure time of 20 ms<sup>(11)</sup>.

To obtain a quantitative reference values, we employed a laboratory-made MO spectrometer system with a retardation modulation technique using a PEM<sup>(9),(10)</sup>.

**2.2 MO Images of Patterned Garnet Films** We have prepared Bi- and Ga-substituted yttrium iron garnet (YIG) thin films by a metal-organic decomposition (MOD) method<sup>(12)</sup>. The samples exhibit magnetization perpendicular to the film plane. In order to investigate the resolution of the magneto-optical contrast, the garnet thin film was patterned into square dot arrays using a photolithography. The size of each dot is  $50 \mu\text{m} \times 50 \mu\text{m}$  in area and 200 nm in thickness, and the separation between dots is 50  $\mu\text{m}$ .

Figures 2(a) and 2(b) show images of Faraday rotation of the garnet dot pattern at the wavelength of 500 nm for opposite directions of remanent magnetization. Corresponding images of Faraday ellipticity are given in Figs. 2(c) and 2(d). These images have been reconstructed by applying eqs. (1) and (2) at each pixel point to three images for three different polarization states; i.e., LP, LCP and RCP. The magnetic contrast between the glass and the garnet portions clearly reversed corresponding to a magnetization reversal. In addition to the magnetic contrast, quantitative values of  $\theta_F$  and  $\eta_F$  can be obtained at any pixel point on the image.

Thus, the present technique provides a quantitative magnetic contrast even in inhomogeneous samples consisting of different

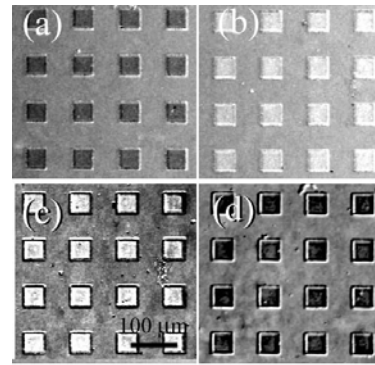


Fig. 2. (a) and (b) are Faraday rotation images, and (c) and (d) Faraday ellipticity images with opposite remanent states. A rotation image and an ellipticity image were obtained from same images for LP, LCP and RCP.

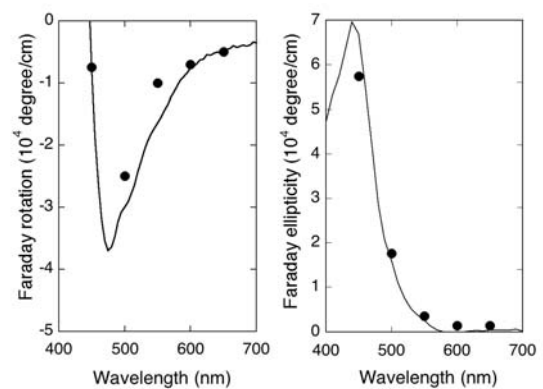


Fig. 3. (a) Faraday rotation and (b) Faraday ellipticity spectra. Solid curves show spectra measured using a conventional MO-spectrometer in an unpatterned film, and dots show data measured by the present MO microscope.

portions with different transmittance. This is in contrast to the conventional crossed polarizer method, which fails to provide quantitative MO values, since the contrast is given only as a difference in optical intensities. The values of  $\theta_F$  and  $\eta_F$  measured using a set of bandpass interference filters in the wavelength range between 450 and 650 nm are plotted by closed circles in Fig. 3 together with the spectra of an unpatterned film measured using the MO spectrometer (solid curves). As observed in the figure, MO values measured by the MO microscope are found to show a remarkable agreement with those measured by the MO spectrometer.

Since most magnetic materials are not transparent, the measurement of Kerr effect is important for practical use. Figure 4 shows magnetic field-dependences of Kerr rotation at wavelength of 500 nm for two different portions: one a garnet pattern portion and a glass substrate portion as shown in an inset.

Once MO images are acquired for a sequence of magnetic field swinging between negative and positive magnetic saturation, hysteresis curves at any pixel point can be visualized only by clicking at the point. As shown in Fig. 4, a clear hysteresis loop is observed at the patterned garnet position, while no signal was observed at the glass substrate position.

In the polarization modulation method, a spatial resolution in MO images is limited by an optical diffraction. A spatial

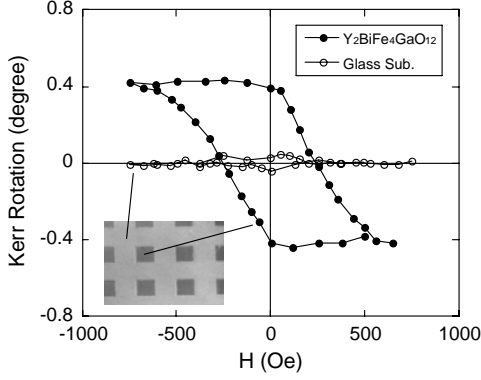


Fig. 4. Magnetic field dependences of Kerr rotation for the garnet dot and the glass substrate.

resolution in the MO images was estimated to be  $0.5 \mu\text{m}$ , consistent with that expected from the value of NA of the objective lens, Mitsutoyo G Plan APO  $\times 50$ , with  $\text{NA}=0.5$ .

The sensitivity in MO images is mainly limited by a shot noise generated in the CCD device. We carried out two kinds of averaging procedures in order to improve the signal to noise ratio (SNR). One is an averaging by accumulation of repeated data at each pixel point, and the other is an averaging over 9 pixel points including 8 pixels surrounding the pixel of concern. An averaging over 100 and 1000 images gives us a noise with a standard deviation of  $0.008^\circ$  and  $0.005^\circ$  for the angle of rotation.

### 3. Magnetic Imaging

**3.1 MO Indicator Films** The MO microscope combined with an MO indicator film allows us to observe a magnetic flux distribution and/or a current distribution in materials even if a sample itself lacks an MO effect. As described before, we used as an MO indicator a Bi-substituted iron garnet film,  $\text{Y}_2\text{BiFe}_5\text{O}_{12}$  (Bi:YIG) with an in-plane anisotropy prepared by the MOD method. The MOD method is favorable not only for the homogeneity of a thin film, the controllability of composition, and the formation of large area, but for the good productivity, since the method makes use of a quite simple procedure, i.e. a spin-coating of solution containing constituent elements followed by an annealing. Detail of film preparation by the MOD method have been described in ref.(12). A Pt mirror layer with a thickness of 100 nm was deposited on the garnet film by a magnetron sputtering method in order to obtain high reflectivity and to avoid scattering of the light due to the pattern fabricated on the sample.

Figure 5 plots the value of Faraday rotation of the indicator film as a function of the magnetic field applied perpendicular to the film plane. The easy-axis of the Bi:YIG film has been confirmed to lie in-plane by VSM measurements. Then the out-of-plane component of magnetization increases linearly with the field until it saturates at an applied field of around 1 kOe. This leads to a linear dependence of the Faraday rotation on the applied field, which allows calibration of the magnitude of magnetic flux for each pixel from the values of the MO rotation.

Next, we will show that the MOD-grown garnet film is more suitable for use as an MO-indicator than a liquid phase epitaxial (LPE) film. Figures 6(a) and 6(b) show MO images of a superconducting Nb film measured with an indicator of the LPE garnet film and the MOD garnet film, respectively. The size of the

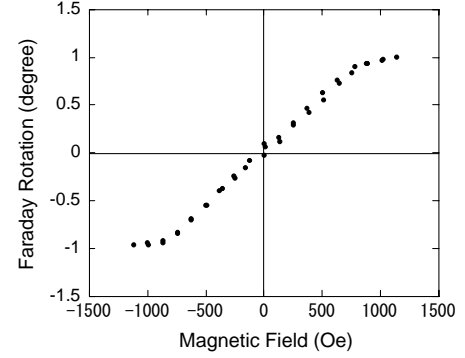


Fig. 5. Magnetic field dependence of Faraday rotation of Bi:YIG film measured at a wavelength of 500 nm.

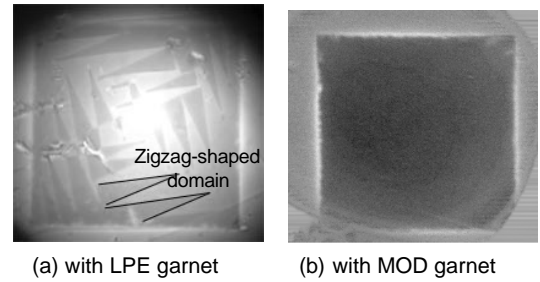


Fig. 6. MO images of a superconducting Nb film measured with (a) LPE film and (b) MOD film as an indicator.

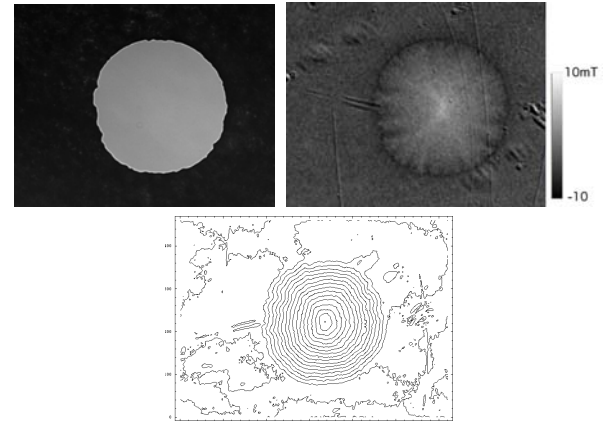


Fig. 7. (a) An optical image and (b) an MO image of  $\text{MgB}_2$  circular pattern with a diameter of  $500 \mu\text{m}$ . Current flow image of  $\text{MgB}_2$  circle pattern deduced from MO image shown in (b).

Nb film is  $0.9 \text{ mm} \times 0.9 \text{ mm}$  in area and 200 nm in thickness. The temperatures of measurement is 4 K, sufficiently lower than the critical temperature ( $\sim 9 \text{ K}$ ) of the Nb film. The images in Figs. 6(a) and 6(b) are showing Meissner state under an applied magnetic field of 16 and 26 Oe, respectively. Thickness of the LPE grown garnet and the MOD grown garnet used in this experiment is  $2 \mu\text{m}$  and 800 nm, respectively. It is found that with a use of the LPE garnet the image suffers zigzag-shaped magnetic domains appearing in the garnet, while with the MOD garnet no such domain structure appears, which allows us to observe the flux distribution clearly. It is thus concluded that the Bi:YIG films grown by MOD method is suitable for MO imaging. Further details are described in Ref. (13).

**3.2 MO Images of Superconductors** MO images of superconducting MgB<sub>2</sub> film were measured using the MO microscope with the Bi:YIG indicator film which covers directly the sample placed in a cryostat equipped with an electro-magnet. The MgB<sub>2</sub> film of 100 nm in thickness was grown by a molecular beam epitaxy (MBE) method<sup>(16)</sup> and was patterned into circular shape of 500 μm in diameter. MO images were measured at 3.9 K with different magnetic fields after zero-field cooling.

Figure 7(a) shows an optical microscope image of the patterned MgB<sub>2</sub>, while Fig. 7(b) shows an MO image at a remanent state after application and removal of magnetic field of 735 Oe. A gradient of the magnetic flux density is clearly observed in the MO image. The contrast in the image corresponds to a density of magnetic flux intruding into the superconductor.

From the MO image, a current distribution can be calculated taking into account the Biot-Savart's law. Figure 7(c) shows a current flow image calculated using the convolution theorem<sup>(17)</sup>, where the contour line indicates a current flow and the density of contour lines corresponds to a current density. The current density deduced from the figure amounts to as high as  $6 \times 10^7$  A/cm<sup>2</sup>, which is consistent with an electrical measurement.

#### 4. Conclusion

We have developed an MO microscope using the polarization modulation technique. Quantitative MO imaging was demonstrated for patterned Bi,Ga:YIG films, and spectra and hysteresis measurements were also demonstrated. In addition, it is found that the quantitative MO imaging technique combined with an MO indicator film is useful to measure magnetic flux images in samples that show no MO effects. Magnetic flux distribution and current flow images were successfully obtained in a patterned superconductor film.

#### Acknowledgement

This work has been supported in part by the Grant-in-Aid for Scientific Research, Basic Research B (No.16360003) from the Japan Society for Promotion of Science. We thank Dr. H. Shibata of NTT basic Research Laboratory and Prof. M. Naito of Tokyo Univ. of Agriculture and Technology for providing MgB<sub>2</sub> samples. We also thank Prof. T. H. Johansen and Dr. J. I. Vestgård of Univ. of Oslo for the calculation of current images. (Manuscript received on December 25, 2007 and revised on February 8, 2008)

#### References

- (1) S. A. Crooker, M. Furis, X. Lou, C. Adelman, D. L. Smith, C. J. Palmström, P.A. Crowell: "Imaging Spin Transport in Lateral Ferromagnet/Semiconductor Structures", *Science*, Vol.309, pp.2191-2195 (2005).
- (2) M. Yamanouchi, D. Chiba, F. Matsukura, and H. Ohno: "Current-induced domain-wall switching in a ferromagnetic semiconductor structure", *Lett. Nature*, Vol.428, pp.539-542 (2004).
- (3) S. Gotoh, N. Koshizuka, M. Yoshida, M. Murakami, and S. Tanaka: "Direct Observation of Flux Behavior in High-Tc Oxide Superconductors Using the Faraday Effect of Iron Garnet Films", *Jpn. J. Appl. Phys.*, Vol.29, L1083-L1085 (1990).
- (4) M. V. Indenbom, N. N. Kolesnikov, M. P. Kulakov, I. G. Naumenko, V. I. Nikitenko, A. A. Polyanskii, N. F. Vershinin, and V. K. V. Vlasov: "Direct study of magnetic flux penetration and trapping in HTSC", *Physica C*, Vol.166, pp.486-496 (1990).
- (5) P.E. Goa, H. Hauglin, Å.A.F. Olsen, M. Bziljevich, and T.H. Johansen: "Magneto-optical imaging setup for single vortex observation",

- Rev. Sci. Instrum.*, Vol.74, pp. 141-146 (2003).
- (6) Y. Martin, D. Rugar, and H. K. Wickramasinghe: "High-resolution magnetic imaging of domains in TbFe by force microscopy", *Appl. Phys. Lett.*, Vol.52, 244-246 (1988).
- (7) J. R. Kirtley, M. B. Ketchen, K. G. Stawiasz, J. Z. Sun, W. J. Gallagher, S. H. Blanton, and S. J. Wind: "High-resolution scanning SQUID microscope", *Appl. Phys. Lett.*, Vol.66, pp.1138-1140 (1995).
- (8) A. M. Chang, H. D. Hallen, L. Harriott, H. F. Hess, H. L. Kao, J. Kwo, R. E. Miller, R. Wolfe, and J. van der Ziel, and T. Y. Chang: "Scanning Hall probe microscopy", *Appl. Phys. Lett.*, Vol.61, pp.1974-1976 (1992).
- (9) K. Sato: "Measurement of Magneto-Optical Kerr Effect Using Piezo-Birefringent Modulator", *Jpn. J. Appl. Phys.*, Vol.20, pp.2403-2409 (1981).
- (10) K. Sato, H. Hongu, H. Ikekame, Y. Tosaka, M. Watanabe, K. Takanashi, H. Fujimori: "Magneto-optical Kerr Spectrometer for 1.2-5.9 eV Region and its Application to FePt/Pt Multilayers", *Jpn. J. Appl. Phys.*, Vol.32, pp.989-995 (1993).
- (11) T. Ishibashi, Z. Kuang, S. Yufune, T. Kawata, M. Oda, T. Tani, Y. Iimura, Y. Konishi, K. Akahane, X. R. Zhao, T. Hasegawa, and K. Sato: "Magneto-Optical Imaging Using Polarization Modulation Method", *J. Appl. Phys.*, Vol.100, 093903 (2006).
- (12) T. Ishibashi, A. Mizusawa, M. Nagai, S. Shimizu, K. Sato, N. Togashi, T. Mogi, M. Houchido, H. Sano, and K. Kuriyama: "Characterization of epitaxial (Y,Bi)<sub>3</sub>(Fe,Ga)<sub>5</sub>O<sub>12</sub> thin films grown by metal-organic decomposition method", *J. Appl. Phys.*, Vol.97, 013516 (2005).
- (13) T. Ishibashi, T. Kawata, T. H. Johansen, J. He, N. Harada, and K. Sato: "Magneto-optical Indicator Garnet Films Grown by Metal-organic Decomposition Method", *J. Mag. Soc. Jpn.*, Vol. 31 (2008) to be published.
- (14) X. R. Zhao, N. Okazaki, Y. Konishi, K. Akahane, Z. Kuang, T. Ishibashi, K. Sato, H. Koinuma, and T. Hasegawa: "Magneto-optical Imaging for High-Throughput Characterization of Combinatorial Magnetic Films", *Appl. Surface Science*, Vol. 223, pp.73-77 (2004).
- (15) X.R. Zhao, W.-Q. Lu, S. Okazaki, Y. Konishi, K. Akahane, T. Ishibashi, K. Sato, Y. Matsumoto, H. Koinuma, T. Hasegawa: "High-throughput characterization of Bi<sub>3</sub>Y<sub>3</sub>Fe<sub>5</sub>O<sub>12</sub> combinatorial thin films by magneto-optical imaging technique"; *Applied Surface Science*, Vol.252 pp.2628-2633 (2006).
- (16) K. Ueda and N. Naito: "In-situ growth of superconducting MgB<sub>2</sub> thin films by molecular-beam epitaxy", *J. Appl. Phys.*, Vol.93, pp.2113-2120 (2003).
- (17) Ch. Jooss, R. Warthmann, A. Forkl and H. Kronmüller: "High-resolution magneto-optical imaging of critical currents in YBa<sub>2</sub>Cu<sub>3</sub>O<sub>7-δ</sub> thin films", *Physica C*, Vol.299, pp.215-230 (1998).



**Katsuki Sato** (Member) received the B. E., M.E., and Doctor of Eng. Degree from Kyoto University, Kyoto, Japan, in 1964, 1966, and 1978, respectively. He joined Japan Broadcasting Corporation in 1966. He joined Tokyo University of Agriculture and Technology as an associate professor in 1984, and promoted to a professor in 1989, and assumed a vice president from 2005 to 2007. He is presently a professor in Graduate School of Engineering, Tokyo University of Agriculture and Technology, and a research supervisor of PRESTO Project, Japan Science and Technology Agency. His research includes growth and characterization of magnetic materials, multinary semiconductors and superconducting materials, and magneto-optics. He is a fellow member of the Japan Society of Applied Physics.



**Takayuki Ishibashi** (Nonmember) received the B. E., M.E., and Doctor of Eng. degree from University of Tsukuba, Ibaraki, Japan, in 1991, 1993, and 1995, respectively. He was an assistant professor of Tokyo University of Agriculture and Technology from 1995 to 2007. He is presently an associate professor in Department of Materials Science and Technology, Nagaoka University of Technology. His research includes thin film growth of magnetic materials and superconducting materials, and magneto-optical imaging. He is a member of the Japan Society of Applied Physics, the Magnetic Society of

Japan, the Physical Society of Japan, and the Ceramics Society of Japan.